

3p-orbital character of the e_g subbands arises from sulfur lone-pair orbitals. (3) The major orbital components of the D peaks are metal 4s and 4p orbitals, while those of the E peaks are phosphorus and sulfur orbitals. Thus, the E peaks are associated with the σ_{P-P}^* and σ_{P-S}^* orbitals of $P_2S_6^{4-}$ ions. (4) The densities of state peaks that occur in the energy region below peak A are largely associated with the 3s orbitals of sulfur and phosphorus.

It is clear from Figure 1 that the 4s, 4p bands of Fe^{2+} ions (D) and the antibonding bands of $P_2S_6^{4-}$ ions (E) are too high in energy to be good acceptor levels and be responsible for the apparent absorption edge of $FePS_3$. Thus, the metal 3d-block bands (B and C), which are partially filled¹⁵ with high-spin d^6 ions, must be responsible for the acceptor capability and also for the absorption edge.

Contrary to the expectation of the weak-interaction model,⁸ the widths of the t_{2g} and e_g subbands (2.0 and 1.5 eV, respectively) are not negligible. In addition, the latter have very strong sulfur lone-pair character. All of these indicate that covalent interactions between iron and sulfur are strong. This conclusion is consistent with the observation¹⁶ that the $10D_q/B$ ratios determined for $MnPS_3$ and $NiPS_3$ are exceptionally large, thereby suggesting a high degree of covalent bonding between metal and sulfur atoms.

Unlike the t_{2g} subbands, the e_g subbands have strong sulfur lone-pair character; therefore, the e_g subbands C are a lot more compatible with the valence band A than are the t_{2g} subbands B. Thus, optical absorption from A to C would be very intense compared with that from A to B and would be responsible for the apparent fundamental absorption edge of $FePS_3$. Bands A and C are estimated to be separated by about 1.8 eV, in reasonable agreement with the apparent band gap 1.5 eV of $FePS_3$.^{5a}

The t_{2g} subbands are largely metal 3d orbital in character so that electron addition into these bands would lead to a sensitive change in the properties of M^{2+} ions. On the other hand, metal 3d-orbital character does not dominate in the e_g subbands, so electron addition into these bands may not significantly modify the properties of M^{2+} ions unless the amount of electron addition

is large enough. This aspect might be quite relevant in interpreting the intercalation behavior of $NiPS_3$.⁷

The t_{2g} subbands are primarily metal 3d orbitals in nature, while the e_g subbands are metal 3d orbitals and sulfur lone-pair orbitals in character. Therefore, electron addition into those bands could not fundamentally change the properties associated with the strength of the P-P and P-S bonds such as their stretching vibrational frequencies. In fact, infrared spectra of Li_xFePS_3 and Li_xNiPS_3 show^{5b} that the ν_{P-P} mode appears at a constant frequency (442 and 440 cm^{-1} for Li_xFePS_3 and Li_xNiPS_3 , respectively).

Concluding Remarks

On the basis of the band structure of $FePS_3$ examined in our study, the following qualitative picture may be proposed for the band electronic structures of other MPX_3 compounds: The positions of the valence and conduction bands of $P_2X_6^{4-}$ ions (A and E, respectively) would be little affected by the nature of M^{2+} . With respect to those bands, the positions of the t_{2g} subbands, the e_g subbands, and 4s and 4p bands of M^{2+} ions (B-D, respectively) would shift toward lower and higher energy for metal atoms M on the right and left of Fe, respectively.

From the present study, it is inevitable to conclude that acceptor levels responsible for intercalation reactions of MPX_3 are low-lying partially filled 3d-block bands. It is the optical absorption from the valence band A to the e_g subband C that is responsible for the apparent fundamental absorption edge of MPX_3 with metal ions other than d^{10} .

As already pointed out, one of the two major reasons why metal 3d levels have not been considered as acceptor levels is the apparent observation that chemical intercalation of lithium affects the magnetic properties of MPX_3 very little.^{5d} However, this observation is not unequivocal: Although experimental difficulties are present, magnetic susceptibilities of Li_xNiPS_3 in the paramagnetic region are found to decrease with x .^{5d} Furthermore, the ³¹P study of Li_xNiPS_3 shows^{7a} that nonmagnetic $NiPS_3$ slabs must occur for $x > 0.5$ at least. In view of the present study, it would be difficult to accept that magnetic susceptibilities of MPX_3 would not vary upon lithium intercalation, unless we are dealing with a genuinely new magnetic phenomenon with MPX_3 systems. Further experimental and theoretical studies are in progress to clarify this problem.

Acknowledgment. M.-H.W. is grateful to the Camille and Henry Dreyfus Foundation for a Teacher-Scholar Award. M.-H.W. thanks Dr. Y. Mathey and Dr. R. Clément for a number of invaluable discussions concerning MPX_3 compounds.

Registry No. $FePS_3$, 20642-11-9.

- (15) (a) Whangbo, M.-H. *Acc. Chem. Res.* **1983**, *16*, 95. (b) Whangbo, M.-H. "Extended Linear Chain Compounds"; Miller, J. S., Ed.; Plenum Press: New York, 1979; p 127. (c) Whangbo, M.-H.; Foshee, M. J.; Hoffmann, R. *Inorg. Chem.* **1980**, *19*, 1723. (d) Whangbo, M.-H. *Inorg. Chem.* **1980**, *19*, 1728.
- (16) (a) Boerio-Goates, J.; Francis, A. H. *Inorg. Chem.* **1981**, *20*, 3019. (b) Clément, R.; Garnier, O.; Mathey, Y. *Nouv. J. Chim.* **1982**, *6*, 13.
- (17) Richardson, J. W.; Nieuwpoort, W. C.; Powell, R. R.; Edgell, W. E. *J. Chem. Phys.* **1962**, *36*, 1057.
- (18) Ammeter, J. H.; Bürgi, H.-B.; Thibault, J. C.; Hoffmann, R. *J. Am. Chem. Soc.* **1978**, *100*, 3686.
- (19) Hinze, J.; Jaffé, H. H. *J. Am. Chem. Soc.* **1962**, *84*, 540.

Notes

Contribution from the Department of Chemistry and the Center for Solid State Science, Arizona State University, Tempe, Arizona 85287

Reaction of Potassium Vapor with Tungsten Trioxide Crystals

D. A. Rieck and L. Eyring*

Received June 26, 1984

Tungsten trioxide is a crystalline solid composed of corner-shared WO_6 octahedra in an essentially cubic array. Ternary compounds with potassium, tungsten, and oxygen are numerous and varied in structure.¹⁻¹⁰ In the tungstates, $K_2W_nO_{3n+1}$, tungsten

has a formal +6 valence. In the nonstoichiometric bronzes, K_xWO_3 , valence varies according to the amount of potassium incorporated into a somewhat complex hexagonal or tetragonal corner-shared WO_6 octahedral network. Two bronzes of interest

- (1) Tanisaki, S. *J. Phys. Soc. Jpn.* **1960**, *15*, 537.
- (2) Loopstra, B. O.; Rietfeld, H. M. *Acta Crystallogr., Sect. B: Struct. Crystallogr. Cryst. Chem.* **1969**, *B25*, 1420.

- (3) Tilley, R. J. D. *Chem. Scr.* **1978-1979**, *14*, 147.
- (4) Ekstrom, T.; Tilley, R. J. D. *Chem. Scr.* **1980**, *16*, 1.
- (5) Okada, K.; Morikawa, H.; Marumo, F.; Iwai, S. *Acta Crystallogr., Sect. B: Struct. Crystallogr. Cryst. Chem.* **1976**, *B32*, 1522.
- (6) Okada, K.; Marumo, F.; Iwai, L. *Acta Crystallogr., Sect. B: Struct. Crystallogr. Cryst. Chem.* **1978**, *B34*, 3193.
- (7) Hussain, A.; Kihlborg, L.; Klug, A. *J. Solid State Chem.* **1978**, *25*, 189.
- (8) Hyde, B. G.; O'Keeffe, M. *Acta Crystallogr., Sect. A: Cryst. Phys., Diffraction, Theor. Gen. Crystallogr.* **1973**, *A29*, 243.
- (9) Iijima, S.; Allpress, J. G. *Acta Crystallogr., Sect. A: Cryst. Phys., Diffraction, Theor. Gen. Crystallogr.* **1979**, *A30*, 22.
- (10) Iijima, S.; Allpress, J. G. *Acta Crystallogr., Sect. A: Cryst. Phys., Diffraction, Theor. Gen. Crystallogr.* **1979**, *A30*, 29.
- (11) Obagashi, H.; Anderson, J. S. *J. Solid State Chem.* **1976**, *17*, 79.



Figure 1. Polished cross section of a crystal of tungsten trioxide, reacted with potassium at 190 °C for 48 h. The width of the area shown is 10 μm .

here are the hexagonal tungsten bronze (HTB), $0.18 \leq x \leq 0.33$, and the tetragonal tungsten bronze (TTB), $0.43 \leq x \leq 0.57$. In the usual methods of preparation, oxides or carbonates of potassium are reacted with oxides of tungsten. This note relates the results of direct reduction of tungsten trioxide by potassium vapor.¹² The attack is extensive but with limited compound formation under the conditions of these experiments.

The purpose of these experiments is to study some microstructural aspects of solid-state reactions in which the structure must transform to include a new metal species in the product structure. Since tungsten trioxide and potassium tungsten bronzes intergrow coherently, it was thought that bronze formation in tungsten trioxide at an inward-moving boundary might be observed under the conditions used. The reaction $\text{K}(\text{vapor}) + \text{WO}_3 = \text{K}_x\text{WO}_3$ was chosen for its chemical simplicity and because the products and reactants are both well characterized by transmission electron microscopy.

Experimental Section

Crystals of tungsten trioxide were grown by heating the powder to 1350 °C for 41 h in an open, platinum-lined quartz tube.¹³ Several of these small crystals (approximately 0.2–0.4 mm on an edge) and 0.1 g of potassium were sealed into evacuated quartz tubes. The resulting capsules were 4–5 cm long and 0.8 cm in diameter. The capsules were tilted and shaken until the crystals were separated 1–2 cm from their platinum holder before placing them horizontally in a boat in a tube furnace. Thirty-four capsules were heated at temperatures between 200 and 950 °C for between 0.25 and 168 h. The partial pressure of the reactant potassium was fixed by the temperature in the capsule. The maintenance of the capsule integrity depended on the charge of potas-

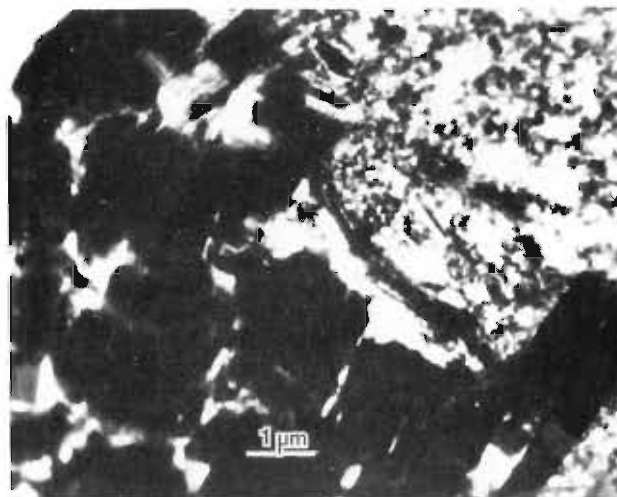


Figure 2. Thin section of another crystal from the same run as Figure 1, set in epoxy resin and cut with a microtome. The left area is tungsten trioxide; the right is the yellow powder.

sium, the temperature, and the duration of the experiment. The products of reaction were analyzed by an electron microprobe and by optical and electron microscopy.

Results

Some of the tungsten trioxide crystals to be reacted were observed in a petrographic microscope. Observation under polarized light revealed some planar faulting along the nearly equivalent $\langle 100 \rangle$ directions. (The $\{100\}$ planes are also cleavage planes.) After reaction, polished cross sections of crystals had the appearance shown in Figure 1. Uneven but parallel gray streaks were observed to penetrate the crystal several microns along $\{100\}$ planes. Microprobe analysis of the streaked region showed a potassium content of about 4.5 mol %, but magnification of 1000 \times revealed that the streaks were rippled on a much finer scale than the width of the microprobe beam; hence, the potassium content of the gray material was considerably more than 4.5 mol %. Since the sample-polishing procedure involved repeated ultrasonic cleaning under water, it is presumed that the potassium is present as a water-insoluble bronze or tungstate.

With a longer reaction time, a higher temperature, or greater access of potassium vapor to the tungsten trioxide crystals, a layer of potassium-containing yellow powder of increasing depth forms on the surface. The boundary between this yellow powder and the green, unreacted tungsten trioxide appears sharp even at 1000 \times magnification in the petrographic microscope, but a gap, rather than a boundary, is seen at a magnification of about 15000 \times in an electron microscope as illustrated in Figure 2.

An X-ray diffraction pattern of the yellow powder is identical with one of tungsten trioxide, even though elemental analysis in the electron microscope (Philips 400 fitted with a Tracor X-ray analysis system) shows it to contain about 12% potassium. The occurrence of the gray penetrating and banded streaks in the less reacted material and the presence of the powder-crystal gap in more completely reacted crystals suggests that the potassium reacts slowly at the surface but penetrates more quickly along the $\{100\}$ cleavage planes. Bronze formation along these planes contributes to faulting and the disintegration of the surface layer of the tungsten trioxide crystal into a layer of unreacted tungsten trioxide powder, with some faces of the powder grains covered by a thin layer of a K-WO_3 compound.

Figure 3 provides a close look at a reaction interface from a sample heated to 925 °C for 15 min. The image shows $[100]$ tungsten trioxide lattice fringes on the right and spacings slightly less than 13 Å that are thought to be $\{100\}$ TTB lattice fringes in the lower left. The dots between the fringes are also about 13 Å apart, as would be expected for a tilted TTB $[001]$ image. In this micrograph the TTB fringes are parallel to the $[120]$ direction of the tungsten trioxide lattice, consistent with the intergrowth of TTB and tungsten trioxide previously proposed.⁸ Unfortunately,

(12) Rieck, D. A. Ph.D. Dissertation, Arizona State University, Dec 1982.
 (13) Lefkowitz, L.; et al. *J. Solid State Chem.* **1975**, *15*, 24.

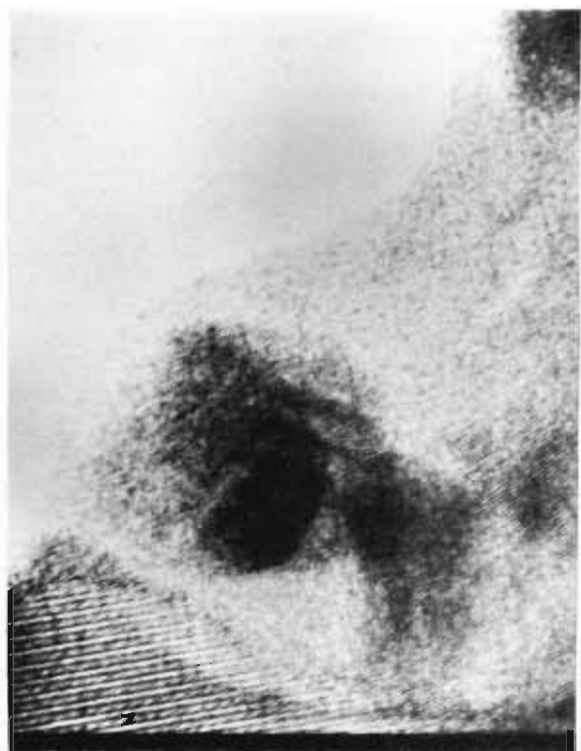


Figure 3. Crystal reacted with potassium at 925 °C for 15 min, showing approximately 13-Å fringes thought to be TTB (lower left) and tungsten trioxide fringes.

the carbon film that supports the crystal seriously reduces the quality of the image.

There is also clear evidence of the formation of tungsten bronze crystals by a vapor reaction. Needlelike or prismatic crystals are found among the tungsten trioxide fragments in the ratio of about 1:100, in a sample heated to 480 °C for 69 h. High-resolution transmission electron microscope images of these needles appear to be *a*-axis projections of both HTB and TTB crystals. This is a growth habit reported for TTB.¹⁴ Hexagonal potassium tungsten bronzes are more often flakes,¹⁵ though Rb_xWO_3 is prismatic.¹⁶ Since these crystals were only a few hundred angstroms wide and 1 μm long, it was not possible to orient them along other axes for an unambiguous identification. The presence of crystals of the appropriate colors and compositions for HTB and TTB in this sample was confirmed by optical microscopy and microprobe analysis.

Discussion

At least two distinct reaction mechanisms operate to produce the bronze phase. One mechanism is vapor growth of needlelike single crystals. The focus of this study is, however, on the second mechanism, a potassium vapor attack on WO_3 crystals.

The interface pictured in Figure 3 is not likely to have been formed by vapor-phase epitaxial growth of TTB on the tungsten trioxide substrate, because of the lack of a sharp crystalline interface. Assuming that the correct orientation match between the TTB and tungsten trioxide is not coincidental, the best explanation would appear to be that potassium bonded to the surface of the crystal, and diffusing from the lower left and moving right, converted the tungsten trioxide to bronze in a surface reaction. The disordered region at the interface is in transition from tungsten trioxide to bronze, as the TTB boundary moves right.

From this study it is clear that whatever process forms the bronzes is kinetically aided by the ease of penetration of potassium along {100} planes. It is also shown that a reaction that appears

to be a simple moving boundary by optical microscopy may actually be more complex.

Acknowledgment. Support by the National Science Foundation through research Grant DMR 81-08306 is gratefully acknowledged. We also thank John Holloway for the use of the optical microscope and his group for instruction in its use. Use of the high-resolution microscope facility was possible through NSF support through Grant DMR-8306501.

Registry No. K, 7440-09-7; WO_3 , 1314-35-8; K_xWO_3 , 37349-36-3.

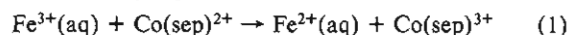
Contribution from the School of Chemical Sciences, University of East Anglia, Norwich NR4 7TJ, England

Kinetics of the Electron-Transfer Reaction between the Hexaquoiron(III) Ion and the Cobalt(II) Sepulchrate Ion

Nigel Rudgwick-Brown and Roderick D. Cannon*

Received May 25, 1983

As part of a study of electron-transfer kinetics of polynuclear complexes, we have examined the reactions of aqueous iron(III) with cobalt(II) sepulchrate,^{1,2} with a view to detecting reaction pathways of the type $\text{Fe}_x(\text{OH})_y^{(3x-y)+} + \text{Co}(\text{sep})^{2+}$.³ In fact, reactions of hydroxo species proved to be too rapid to follow at the iron concentrations required to achieve significant polymerization. Acceptable data were however obtained for reaction 1, and these are briefly reported.



Cobalt(II) sepulchrate solutions were prepared by zinc reduction of cobalt(III) sepulchrate^{1b} in neutral aqueous solution under nitrogen and adjusted to the required acidity and ionic strength immediately before use. Measurements were made in the Aminco-Morrow stopped-flow apparatus with precautions against air oxidation.⁴ A constant ionic medium was maintained by using Cr^{3+} to balance variations in Fe^{3+} concentration and Li^+ to balance H^+ . Reactions were carried out with Co/Fe ratios initially in the range 1.25–1.67, but data were taken in the third to fifth half-lives of the reaction (absorbance change typically 0.05) and pseudo-first-order kinetics were observed. Constancy of $k_{\text{obsd}}/([\text{Co}^{\text{II}}]_0 - [\text{Fe}^{\text{III}}]_0)$ and lack of $[\text{H}^+]$ dependence (Table I) indicate the rate law⁵

$$-d[\text{Co}(\text{sep})^{2+}]/dt = k[\text{Fe}^{3+}][\text{Co}(\text{sep})^{2+}] \quad (2)$$

$k = (1.2 \pm 0.1) \times 10^5 \text{ M}^{-1} \text{ s}^{-1}$ at 0 °C, $k = (1.75 \pm 0.2) \times 10^5 \text{ M}^{-1} \text{ s}^{-1}$ at 25 °C, and $I = 0.23 \text{ M}(\text{LiNO}_3)$.

The structure of the sepulchrate ligand ensures that reaction 1 is outer sphere. Rates of outer-sphere reactions are usually explained in terms of the Marcus equations⁸

$$\log k = \frac{1}{2}(\log k_{11} + \log k_{22} + \log K + \log f) \quad (3)$$

$$\log f = (\log K)^2 / (4 \log(k_{11}k_{22}/Z^2)) \quad (4)$$

where K is the equilibrium constant of reaction 1, k_{11} and k_{22} are rate constants of the self-exchange reactions, and Z is a limiting rate constant, corresponding to a diffusion-controlled encounter

(1) (a) Creaser, I. I.; Harrowfield, J. MacB.; Herlt, A. J.; Sargeson, A. M.; Springborg, J.; Geue, R. J.; Snow, M. R. *J. Am. Chem. Soc.* **1977**, *99*, 3181. (b) Harrowfield, J. MacB.; Herlt, A. J.; Sargeson, A. M.; Del Donno, T. *Inorg. Synth.* **1982**, *20*, 85.

(2) Sargeson, A. M. *Chem. Br.* **1979**, *15*, 23.

(3) sep = 1,3,6,8,10,13,16,19-octaazaabicyclo[6.6.6]icosane.

(4) Rudgwick-Brown, N.; Cannon, R. D. *J. Chem. Soc., Dalton Trans.* **1984**, 479.

(5) Under the conditions used, not more than 0.004% of the iron(III) is present as $\text{Fe}_2(\text{OH})_2^{4+}$ (calculated from data of ref 7, Table 2).

(6) Baes, C. F.; Mesmer, R. E. "The Hydrolysis of Cations"; Wiley: New York, 1976; Table 10.18.

(7) Sillén, L. G.; Martell, A. E. "Stability Constants of Metal-Ion Complexes"; The Chemical Society: London 1964; Spec. Publ. No. 17.

(8) Marcus, R. A. *J. Chem. Phys.* **1965**, *43*, 679.

(14) Magnéli, A. *Ark. Kem.* **1949**, *1*, 213.

(15) Magnéli, A. *Acta Chem. Scand.* **1953**, *7*, 315.

(16) Wanlass, D. R.; Sienko, M. J. *J. Solid State Chem.* **1975**, *12*, 362.